Journal of Clinical and Translational Hepatology **2026** | Epub
DOI: 10.14218/JCTH.2026.00370

Original Article

KPNB1 Promotes Cholangiocarcinoma Progression through LDHA Nuclear Translocation and SOX2 Activation

Fangqian Du[1#], Xiangyan Zhang[2#], Yuwei Xie[1], Hao Zou[1], Kun Li[1], Kui Liu[1], Praveena George[3], Bingzi Dong[4*] and Chengzhan Zhu[1,5*]

[1]*Department of Hepatobiliary and Pancreatic Surgery, The Affiliated Hospital of Qingdao University, Qingdao, Shandong, China;* [2]*Department of Pathology, The Affiliated Hospital of Qingdao University, Qingdao, Shandong, China;* [3]*Department of Biology, University of Massachusetts Amherst, Amherst, MA, USA;* [4]*Department of Endocrinology and Metabolism, The Affiliated Hospital of Qingdao University, Qingdao, Shandong, China;* [5]*Shandong Key Laboratory of Digital Medicine and Computer Assisted Surgery, The Affiliated Hospital of Qingdao University, Qingdao, Shandong, China*

[#]*Contributed equally to this work.*

Received: May 12, 2026 | **Revised:** August 13, 2026 | **Accepted:** October 21, 2026 | **Published online:** November 17, 2026

Abstract

Background and Aims: Extrahepatic cholangiocarcinoma (eCCA) is often accompanied by biliary obstruction and alterations in bile composition, which may affect the tumor microenvironment. KPNB1 is a key nuclear transport receptor that is aberrantly expressed in various malignancies. However, KPNB1's role in cholangiocarcinoma (CCA) remains unclear. In this study, we aimed to investigate the biological role and underlying molecular mechanisms of KPNB1 in CCA progression and explore its association with the biliary microenvironment.

Methods: To investigate the role of KPNB1 in CCA, we analyzed its expression and clinical significance using public databases and clinical specimens and performed a series of *in vitro* and *in vivo* functional experiments. The antitumor effects of the KPNB1 inhibitor importazole were assessed *in vitro* and *in vivo*. The KPNB1-LDHA-SOX2 signaling pathway was investigated using mass spectrometry, immunoprecipitation, and rescue assays. Furthermore, KPNB1 levels in bile were analyzed, and their clinical value was evaluated.

Results: KPNB1 was markedly overexpressed in eCCA tissues and was associated with aggressive clinicopathological features and poor prognosis. Functional analyses demonstrated that KPNB1 enhanced CCA cell proliferation, migration, invasion, epithelial–mesenchymal transition, and stemness-related characteristics of CCA cells, whereas importazole significantly inhibited these malignant phenotypes and tumor growth. Mechanistically, KPNB1 enhanced the expression of stemness-related genes by promoting the nuclear accumulation of LDHA and its interaction with SOX2. Furthermore, eCCA-derived bile enhanced malignant phenotypes and KPNB1 protein expression in CCA cells, while eCCA bile-derived exosomes were enriched in KPNB1 and exerted similar tumor-promoting effects.

Conclusions: KPNB1 promotes cholangiocarcinoma progression through the KPNB1-LDHA-SOX2 axis and may contribute to tumor progression within the biliary microenvironment. Elevated KPNB1 levels in bile may have potential prognostic value, and targeting KPNB1 may represent a promising therapeutic strategy for cholangiocarcinoma.

Keywords: Extrahepatic cholangiocarcinoma; Bile; Nuclear translocation; KPNB1; Cell stemness; LDHA; SOX2.
***Correspondence to:** Chengzhan Zhu, Department of Hepatobiliary and Pancreatic Surgery, The Affiliated Hospital of Qingdao University, Qingdao, Shandong 266003, China. ORCID: https://orcid.org/0000-0002-2775-5863. Tel: +86-532-82919552, E-mail: zhuchengz@qduhospital.cn; Bingzi Dong, Department of Endocrinology and Metabolism, The Affiliated Hospital of Qingdao University, Qingdao, Shandong 266003, China. ORCID: https://orcid.org/0000-0003-2446-0725. Tel: +86-532-82911383, E-mail: dongbingzi@hotmail.com.
How to cite this article: Du F, Zhang X, Xie Y, Zou H, Li K, Liu K, *et al*. KPNB1 Promotes Cholangiocarcinoma Progression through LDHA Nuclear Translocation and SOX2 Activation. *J Clin Transl Hepatol*. Published online: Nov 17, 2026. DOI: 10.14218/JCTH.2026.00370.

Introduction

Cholangiocarcinoma (CCA) is an aggressive malignancy of the biliary epithelium and the second most common primary liver cancer after hepatocellular carcinoma.[1] Despite advances in targeted therapies and immunotherapy, clinical outcomes remain poor, largely owing to late-stage presentation and a high risk of recurrence after curative-intent resection.[2] Anatomically, CCA is classified into two subtypes: intrahepatic (iCCA) and extrahepatic (eCCA). eCCA is frequently accompanied by biliary obstruction

© 2026 The Author(s). This article has been published under the terms of Creative Commons Attribution-Noncommercial 4.0 International License (CC BY-NC 4.0), which permits noncommercial unrestricted use, distribution, and reproduction in any medium, provided that the following statement is provided. "This article has been published in *Journal of Clinical and Translational Hepatology* at https://doi.org/10.14218/JCTH.2026.00370 and can also be viewed on the Journal's website at https://www.xiahepublishing.com/journal/jcth".

and obstructive jaundice, resulting in persistent cholestasis and profound alterations in bile composition. These pathological changes expose tumor cells to a distinct biliary microenvironment that may influence disease progression and therapeutic response.[3,4]

The biliary tract maintains bile secretion and flow, while biliary epithelial cells are continuously exposed to the biochemical and microbial milieu of bile. Bile acids, inflammatory mediators, metabolites, and microbial products can influence epithelial inflammatory responses, metabolic homeostasis, and tumor-associated signaling pathways.[5-7] In the setting of biliary obstruction, cholestasis disrupts bile acid homeostasis and promotes oxidative stress and inflammatory signaling, conditions that may favor CCA progression.[4,8] Moreover, extracellular vesicles present in bile may mediate cellular crosstalk and have shown promise as novel biomarkers for the diagnosis and prognosis of cholangiocarcinoma.[9-12] However, how these dynamic components of the biliary microenvironment interact with tumor cells to promote CCA progression remains poorly defined.

Aberrant nucleocytoplasmic transport is considered a hallmark of tumor development and progression. Disruption of this process can result in the aberrant subcellular localization of oncogenic proteins and tumor suppressors, thereby influencing key processes such as cell proliferation, metabolic reprogramming, and transcriptional regulation.[13] Karyopherin subunit beta 1 (KPNB1) functions as an essential receptor in the classical nucleocytoplasmic transport system, primarily facilitating the nuclear import of proteins harboring nuclear localization signals.[14,15] Emerging evidence indicates that KPNB1 contributes not only to canonical nuclear transport but also to multiple malignant behaviors, such as enhanced tumor proliferation,[16,17] epithelial–mesenchymal transition (EMT),[18] and resistance to anticancer therapy.[19] KPNB1 is frequently overexpressed in multiple solid tumors and promotes tumor progression by facilitating the nuclear translocation of key oncogenic proteins.[20,21] For instance, KPNB1 facilitates the nuclear import of molecules including PD-L1, YBX1, and NF-κB, thereby promoting tumor progression.[22-24] However, the biological role of KPNB1 in cholangiocarcinoma remains poorly understood. Moreover, whether KPNB1 responds to bile-derived signals and how it mediates downstream oncogenic events in cholangiocarcinoma remain largely unknown.

Given the evidence described above, the present study sought to investigate the biological role and underlying molecular mechanisms of KPNB1 in cholangiocarcinoma. In addition, this study explores the potential involvement of bile in KPNB1-mediated oncogenic signaling. These findings may further elucidate the molecular basis of CCA progression and offer a potential rationale for the development of KPNB1-targeted therapeutic approaches.

Methods

Bioinformatics

Pan-cancer expression of KPNB1 was analyzed using the UALCAN database (https://ualcan.path.uab.edu). RNA-sequencing data for cholangiocarcinoma, comprising 35 tumors and nine normal tissues, were obtained from The Cancer Genome Atlas (TCGA) (https://portal.gdc.cancer.gov). Protein interaction partners of LDHA were predicted using HitPredict and STRING (https://www.hitpredict.org/; https://cn.string-db.org/).

Cell culture and transfection

HUCCT1 and QBC939 cell lines (Shanghai Institute of Biological Sciences, Chinese Academy of Sciences) were cultured in RPMI-1640 and DMEM (Hyclone, USA), respectively. The media were supplemented with 10% fetal bovine serum (Vivacell, China). Cells were maintained at 37 °C in a 5% CO_2 incubator. The cell lines were authenticated by short tandem repeat analysis and confirmed to be free of mycoplasma contamination using a mycoplasma detection kit (Vazyme, D201).

Small interfering RNAs (siRNAs) targeting KPNB1, LDHA, SOX2, and control siRNA were purchased from GenePharma (China) and transfected using Xfect RNA reagent (Takara, Japan). The pGL3-Basic-NANOG promoter and pRL-TK plasmids were obtained from GenePPL (China). FLAG-KPNB1, FLAG-LDHA, and FLAG-SOX2 plasmids were obtained from GeneralBiol (China) and transfected using Lipofectamine 3000 (Invitrogen, USA). Stable KPNB1-overexpressing HUCCT1 cells were generated using lentiviral vectors (GeneChem, China), followed by puromycin selection. Importazole (IPZ; MCE, USA) was dissolved in dimethyl sulfoxide (DMSO).[25]

Patients

Tumor tissues and adjacent histologically normal bile duct tissues were collected from patients with eCCA who underwent surgical resection at The Affiliated Hospital of Qingdao University. Immunohistochemical (IHC) analysis was performed on specimens from 50 patients, whereas reverse transcription quantitative PCR (RT-qPCR) analysis was performed on specimens from 40 patients. Bile samples were collected through clinically indicated biliary drainage from 70 patients with histologically confirmed eCCA and 20 patients with gallstones who served as non-malignant controls. Gallstone disease was confirmed by clinical imaging, and biliary tract malignancy was excluded in all control patients. For *in vitro* bile treatment experiments, each functional assay included bile samples from at least 10 independent patients. Written informed consent was obtained from all participants. This study was approved by the Institutional Ethics Committee of The Affiliated Hospital of Qingdao University (Approval No. QYFYWZLL30901) and was conducted in accordance with the Declaration of Helsinki (as revised in 2024).

Reverse transcription quantitative PCR (RT-qPCR)

Total RNA was extracted using RNA Release Easy reagent (Vazyme, China), reverse-transcribed into complementary DNA (cDNA), and analyzed by quantitative reverse transcription PCR (RT-qPCR) using SYBR Green chemistry on a LightCycler 480 II system (Roche). GAPDH was used as the internal control gene.[26] Primer sequences are listed in Supplementary Table 1.

Cell viability and colony formation assays

Cell growth was assessed using a Cell Counting Kit-8 (CCK-8) (MeilunBio, China).[26] Approximately 2×10^3 cells were seeded into each well of 96-well plates. Following incubation with CCK-8 working solution at 37°C, the optical density (OD) at 450 nm

was measured daily for five consecutive days.

For the colony formation assay,[26] 1×10^3 cells were seeded in six-well plates and cultured for 14 days. The resulting colonies were subsequently fixed and stained with 0.1% crystal violet.

Wound-healing assay and F-actin staining

Wound-healing assays were performed by creating a linear scratch in confluent cell monolayers.[26] Images were captured at 0 and 48 h, and wound closure was quantified using ImageJ software. F-actin staining was performed according to the manufacturer's instructions (Beyotime, #C2207S). Nuclei were counterstained with DAPI.[26]

Cell migration and invasion assays

CCA cells (1×10^5) suspended in serum-free basal culture medium were seeded into the upper chambers of Transwell inserts, while complete medium supplemented with 10% fetal bovine serum was added to the lower chambers. For invasion assays, the inserts were pre-coated with diluted Matrigel (BD Biosciences, USA). Following incubation, cells that had migrated through the membrane were fixed, stained with crystal violet, and counted in fields under a microscope.[26]

Nuclear, cytoplasmic, and membrane protein separation

Nuclear, cytoplasmic, and membrane proteins were extracted using a Nucleus and Cytoplasmic Protein Extraction Kit (Absin, #abs9346).[27] Briefly, cells were sequentially lysed using cytoplasmic, nuclear, and membrane protein extraction reagents supplemented with phenylmethylsulfonyl fluoride. Following stepwise centrifugation, the corresponding protein fractions were collected separately. Protein concentrations were determined using a bicinchoninic acid (BCA) Protein Assay Kit (Beyotime, #P0010S), followed by Western blot analysis.

Western blotting

Total protein was extracted using RIPA buffer. Equal amounts of protein were separated by SDS-PAGE and transferred onto polyvinylidene difluoride (PVDF) membranes (Merck Millipore). The membranes were incubated with primary antibodies overnight at 4°C, followed by incubation with HRP-conjugated secondary antibodies for one hour at room temperature. Protein bands were visualized using enhanced chemiluminescence (KF005, Affinity Biosciences, USA) and quantified with ImageJ software.[26] Details of the primary antibodies are provided in Supplementary Table 2.

Co-immunoprecipitation (Co-IP)

Cells were lysed in NP-40 buffer (Beyotime Biotechnology, China) supplemented with phenylmethylsulfonyl fluoride and protease inhibitors (MCE, USA). The lysates were collected and centrifuged to remove cellular debris, and the resulting supernatants containing total protein were collected. For immunoprecipitation, magnetic beads (MCE, USA) were incubated with the indicated primary antibodies at the recommended dilution to allow antibody conjugation. The prepared protein lysates were incubated overnight at 4°C with antibody-coupled magnetic beads under gentle rotation to facilitate immune complex formation. The beads were rinsed using binding/wash buffer, and the immunoprecipitated complexes were then mixed with 1× loading buffer (Beyotime Biotechnology, China) and heated at 95°C for five minutes. The eluted proteins were collected and subjected to Western blot analysis.[28]

Dual-luciferase reporter assay

Cells were co-transfected with the NANOG promoter-driven luciferase reporter plasmid, the Renilla luciferase control plasmid, and the indicated expression plasmids or siRNAs. Luciferase activity was measured using a Dual-Luciferase Reporter Assay Kit (Vazyme, DL101-01) according to the manufacturer's instructions. Firefly luciferase activity was normalized to Renilla luciferase activity.[29]

Exosome isolation and uptake

Bile samples were sequentially centrifuged at 4°C (300 ×g for 10 min and 3,500 rpm for 40 min) to remove cells and debris. The samples were then ultrafiltered by centrifugation at 3,500 rpm for 40 min, passed through a 0.22 μm filter membrane, and ultracentrifuged at 110,000 × g for 140 min at 4°C. The resulting exosome pellet was resuspended in PBS buffer, passed through a 0.22 μm filter membrane, and stored at −80°C until use.[10]

Purified exosomes were labeled using PKH67 fluorescent dye (Solarbio, D0031) according to the manufacturer's protocol. The labeled exosomes were incubated with CCA cells, and cellular uptake was observed using fluorescence microscopy.[28]

Enzyme-linked immunosorbent assay (ELISA)

Bile KPNB1 concentrations were quantified using a commercially available human KPNB1 ELISA kit (Ruixinbio, RX2D1008176) according to the manufacturer's instructions. Absorbance at 450 nm was measured using a microplate reader.[30]

In vivo tumor models

Stable KPNB1-overexpressing or vector-control HUCCT1 cells (5×10^6) were subcutaneously injected into 4-week-old male BALB/c nude mice (Beijing Vital River, China; $n = 6$/group). In a separate experiment, mice bearing wild-type HUCCT1 xenografts were randomly assigned to receive IPZ (20 mg/kg, intraperitoneally) or DMSO three times per week for two weeks after tumors reached ~30 mm^3 ($n = 5$/group). Tumor volume was calculated as length × $width^2$ × 0.5. Mice were euthanized when either the maximum tumor diameter reached 20 mm or the tumor volume reached 2,000 mm^3, whichever occurred first. Tumors were subsequently collected for histological analysis.[26]

For the experimental lung metastasis model, control or KPNB1-overexpressing HUCCT1 cells were injected via the tail vein.[31] Two weeks after injection, mice in the KPNB1-overexpression group were randomly assigned to receive IPZ (20 mg/kg, intraperitoneally, three times weekly) or DMSO ($n = 4$/group). Mice were monitored throughout the experiment and euthanized when body weight loss reached 20% of baseline. Pulmonary metastatic burden was assessed by quantifying metastatic nodules. All animal procedures were approved by the Animal Ethics Committee of The Affiliated Hospital of Qingdao University (No. AHQU-MAL20250609DFQ) and conducted in accordance with the Chinese national standard Laboratory animals—General code of animal welfare (GB/T 42011–2022). The animal experiments were reported in accordance with the ARRIVE guidelines.

Statistical analysis

Statistical analyses were performed using GraphPad Prism 8.0

(San Diego, CA, USA). Data are presented as the mean ± standard deviation (SD). Differences between groups were analyzed using Student's t-test, one-way ANOVA, two-way ANOVA, the χ^2 test, or Fisher's exact test, as appropriate. Kaplan–Meier analysis with the log-rank test, Cox proportional hazards regression, and receiver operating characteristic (ROC) curve analysis were performed to evaluate survival and prognostic value. $P < 0.05$ was considered statistically significant.

Results

KPNB1 is upregulated in CCA and is associated with poor prognosis

Pan-cancer analysis using the UALCAN database demonstrated that KPNB1 was significantly upregulated across multiple human malignancies (Fig. 1A). Consistently, analysis of the TCGA cholangiocarcinoma cohort showed markedly higher KPNB1 expression in tumor tissues than in normal bile duct tissues (Fig. 1B). These findings were further confirmed in clinical specimens collected from The Affiliated Hospital of Qingdao University. Immunohistochemistry and RT-qPCR analyses consistently demonstrated significantly higher KPNB1 expression in extrahepatic cholangiocarcinoma tumor tissues than in unpaired adjacent normal bile duct tissues (Fig. 1C–D).

To further investigate the clinical significance of KPNB1, patients were divided into high- and low-expression groups based on the median *KPNB1* mRNA level, and the associations between KPNB1 expression and clinicopathological features were analyzed. High KPNB1 expression was significantly associated with advanced TNM stage ($P = 0.025$) (Supplementary Table 3). Kaplan–Meier survival analysis further demonstrated that high KPNB1 expression was significantly associated with shorter disease-free survival (Fig. 1E). Furthermore, multivariate Cox proportional hazards regression analysis identified high KPNB1 expression as an independent prognostic factor for postoperative recurrence ($P = 0.022$) (Supplementary Table 4).

To further evaluate the clinical applicability of KPNB1, ROC analyses were performed using postoperative recurrence and mortality as clinical endpoints. For predicting postoperative recurrence, KPNB1 yielded an area under the curve (AUC) of 0.720, which was higher than those of carbohydrate antigen 19-9 (CA19-9, 0.629), carcinoembryonic antigen (CEA, 0.519), and alpha-fetoprotein (AFP, 0.520) (Supplementary Fig. 1A). For predicting mortality, KPNB1 yielded an AUC of 0.670, exceeding those of CEA (0.606) and AFP (0.509) and comparable to that of CA19-9 (0.637) (Supplementary Fig. 1B). Collectively, these findings indicate that elevated KPNB1 expression is associated with advanced disease and unfavorable postoperative outcomes in patients with cholangiocarcinoma.

KPNB1 promotes proliferation, migration, invasion, and stemness in CCA cells

To investigate the functional role of KPNB1 in CCA, KPNB1 was overexpressed using plasmid transfection or silenced using siRNA. RT-qPCR confirmed the efficiency of KPNB1 overexpression and knockdown (Fig. 2A, Supplementary Fig. 2A). Colony formation and CCK-8 assays showed that KPNB1 overexpression markedly enhanced cell proliferation, whereas KPNB1 knockdown significantly inhibited proliferation (Fig. 2B–C; Supplementary Fig. 2B–C). Consistently, Transwell and wound-healing assays showed that KPNB1 overexpression promoted cell migration and invasion, while KPNB1 silencing had the opposite effect (Fig. 2E–F, Supplementary Fig. 2E–F). Furthermore, F-actin staining demonstrated that KPNB1 overexpression significantly increased cytoskeletal remodeling and pseudopodia formation in CCA cells, whereas KPNB1 knockdown reduced both phenotypes (Fig. 2G–H, Supplementary Fig. 2G–H).

To assess the effects of KPNB1 on tumor cell stemness, RT-qPCR analysis demonstrated that KPNB1 positively regulated the transcription of stemness-related genes (Fig. 2D, Supplementary Fig. 2D). At the molecular level, Western blot analysis showed that KPNB1 overexpression decreased E-cadherin expression and increased N-cadherin and vimentin expression. Concurrently, the stemness-associated markers, CD133 and CD44, were upregulated (Fig. 2I; Supplementary Fig. 2I), whereas KPNB1 knockdown produced the opposite effects (Fig. 2J, Supplementary Fig. 2J). These findings demonstrate that KPNB1 promotes EMT-associated phenotypes and stemness in CCA cells.

Pharmacological inhibition of KPNB1 suppresses malignant phenotypes of CCA cells

To further evaluate the therapeutic potential of targeting KPNB1, CCA cells were treated with the KPNB1 inhibitor importazole (IPZ) to inhibit KPNB1-mediated nuclear transport.[25] Cell viability assays indicated that IPZ inhibited the growth of HUCCT1 and QBC939 cells in a dose-dependent manner, with IC_{50} values approximately 25 μM (Fig. 3A). Therefore, 25 μM IPZ was selected for subsequent experiments. Functionally, IPZ significantly inhibited cell proliferation, as demonstrated by CCK-8 and colony formation assays (Fig. 3B–C, Supplementary Fig. 3A–B). In addition, Transwell and wound-healing assays showed that IPZ markedly reduced cell migration and invasion (Fig. 3D–E, Supplementary Fig. 3C–D). F-actin staining further showed that IPZ disrupted cytoskeletal organization and reduced pseudopodia formation (Fig. 3F, Supplementary Fig. 3E). IPZ treatment also suppressed the expression of EMT-related proteins (Fig. 3G; Supplementary Fig. 3G) and significantly reduced the expression of stemness-associated proteins CD133 and CD44 (Fig. 3H, Supplementary Fig. 3H), as well as the transcriptional levels of stemness-related genes (Fig. 3I, Supplementary Fig. 3F). Importantly, IPZ treatment partially reversed the enhanced proliferative, migratory, and invasive phenotypes induced by KPNB1 overexpression, further supporting the functional involvement of KPNB1 in CCA progression (Fig. 3J–M, Supplementary Fig. 3I–N).

KPNB1 interacts with LDHA to promote CCA progression

To explore the molecular mechanisms underlying KPNB1-mediated tumor progression, liquid chromatography-tandem mass spectrometry (LC-MS/MS) analysis of proteins co-immunoprecipitated with KPNB1 identified lactate dehydrogenase A (LDHA) as a candidate interacting protein. Co-immunoprecipitation (Co-IP) and Coomassie Brilliant Blue staining supported an interaction between endogenous KPNB1

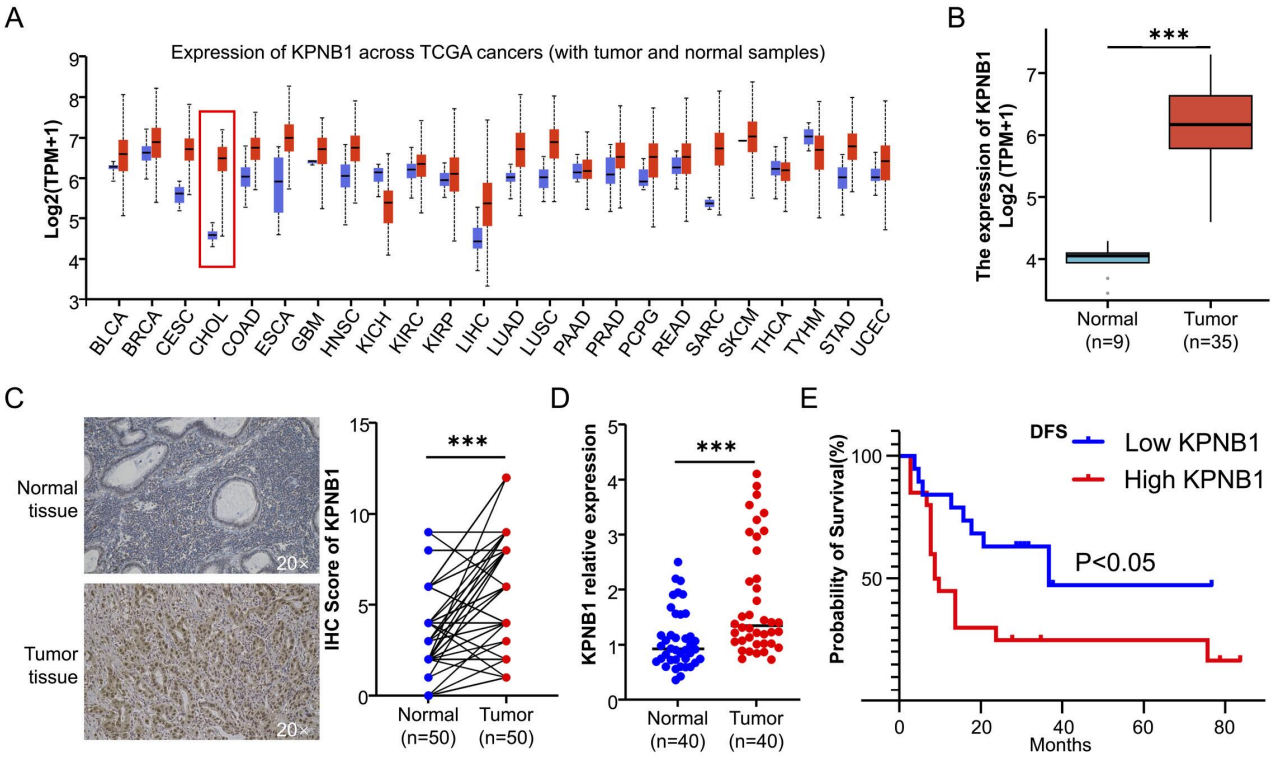


Fig. 1. KPNB1 expression in cholangiocarcinoma and its association with clinical outcomes. (A) Pan-cancer analysis of KPNB1 expression based on the UALCAN database. (B) KPNB1 expression in cholangiocarcinoma tissues (n = 35) and normal tissues (n = 9) from the TCGA-CHOL dataset. (C) Representative immunohistochemical staining (20×) and quantitative analysis of KPNB1 in extrahepatic cholangiocarcinoma (eCCA) tissues and adjacent normal tissues. (D) KPNB1 mRNA expression in eCCA tissues and adjacent normal tissues determined by RT-qPCR. (E) Kaplan–Meier analysis of disease-free survival (DFS) in patients with eCCA stratified according to KPNB1 expression. ***P< 0.001. TCGA, The Cancer Genome Atlas; BLCA, bladder urothelial carcinoma; BRCA, breast invasive carcinoma; CESC, cervical squamous cell carcinoma and endocervical adenocarcinoma; CHOL, cholangiocarcinoma; COAD, colon adenocarcinoma; ESCA, esophageal carcinoma; GBM, glioblastoma multiforme; HNSC, head and neck squamous cell carcinoma; KICH, kidney chromophobe; KIRC, kidney renal clear cell carcinoma; KIRP, kidney renal papillary cell carcinoma; LIHC, liver hepatocellular carcinoma; LUAD, lung adenocarcinoma; LUSC, lung squamous cell carcinoma; PAAD, pancreatic adenocarcinoma; PRAD, prostate adenocarcinoma; PCPG, pheochromocytoma and paraganglioma; READ, rectum adenocarcinoma; SARC, sarcoma; SKCM, skin cutaneous melanoma; THCA, thyroid carcinoma; THYM, thymoma; STAD, stomach adenocarcinoma; UCEC, uterine corpus endometrial carcinoma; TPM, transcripts per million; IHC, immunohistochemistry; eCCA, extrahepatic cholangiocarcinoma; mRNA, messenger RNA; RT-qPCR, reverse transcription quantitative polymerase chain reaction; DFS, disease-free survival.

and LDHA (Fig. 4A–B, Supplementary Fig. 4A). To further evaluate the structural feasibility of this interaction, molecular docking analysis was performed using ClusPro, which suggested a plausible binding interface between KPNB1 and LDHA (Fig. 4C).

To evaluate the functional relevance of this interaction, LDHA was silenced in KPNB1-overexpressing cells (Supplementary Fig. 4B). Functional assays demonstrated that LDHA knockdown significantly attenuated KPNB1-induced cell proliferation (Fig. 4D, Fig. 4G, Supplementary Fig. 4F–G) and reduced cell migration (Fig. 4E–F, Supplementary Fig. 4C–D). In addition, F-actin staining showed that LDHA depletion impaired cytoskeletal remodeling and pseudopodia formation, consistent with reduced cell motility (Fig. 4H, Supplementary Fig. 4E). Collectively, these findings support a role for LDHA as a functional downstream effector of KPNB1 in cholangiocarcinoma.

KPNB1 promotes nuclear accumulation of LDHA

We next investigated whether KPNB1 regulates LDHA expression. Western blot analysis showed that KPNB1 overexpression, KPNB1 knockdown, or IPZ treatment did not significantly affect total LDHA protein levels in CCA cells (Fig. 5A, Supplementary Fig. 5A). Given the role of KPNB1 in nuclear transport,[14] we hypothesized that KPNB1 may regulate the subcellular localization of LDHA. Subcellular fractionation followed by Western blot analysis revealed that KPNB1 overexpression increased the nuclear accumulation of LDHA, whereas KPNB1 knockdown reduced nuclear LDHA levels (Fig. 5B–C, Supplementary Fig. 5B–C). Consistent with these

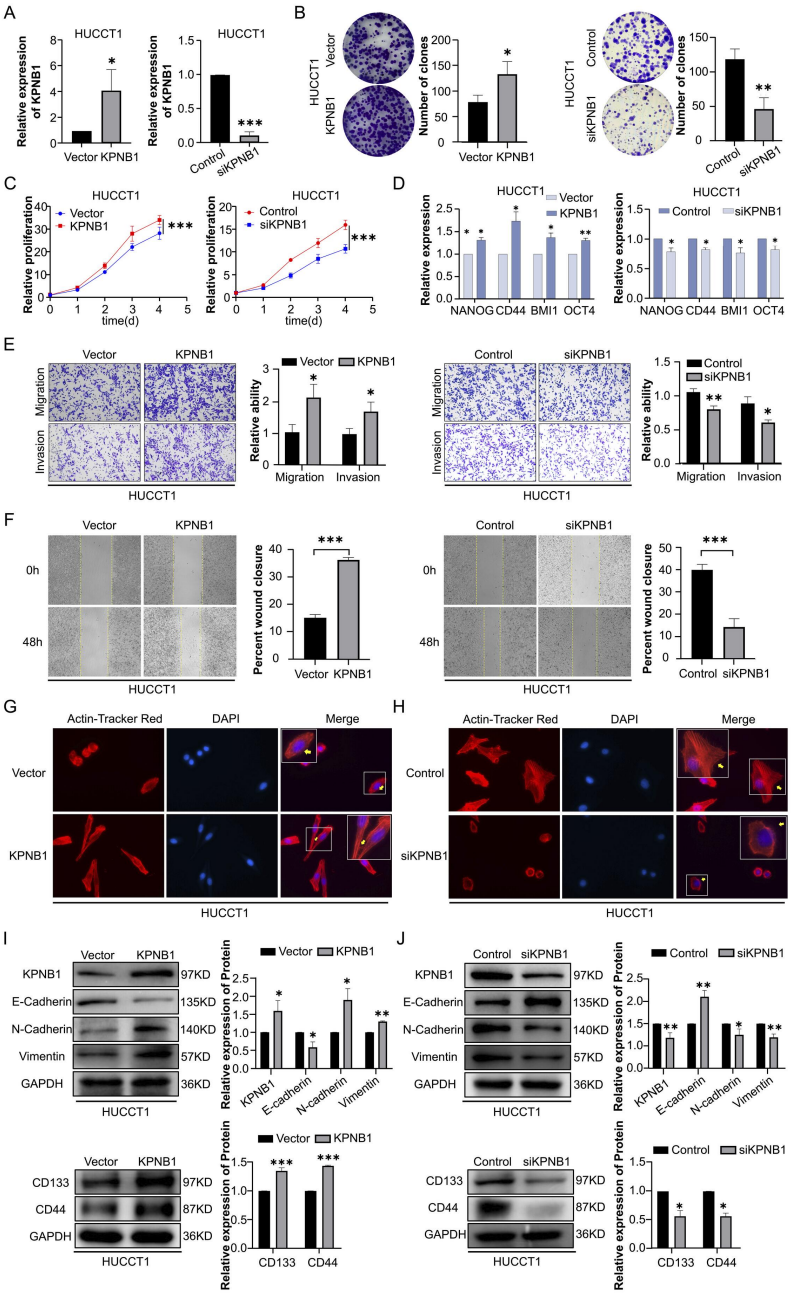


Fig. 2. Effects of KPNB1 expression on malignant phenotypes of cholangiocarcinoma cells. (A) KPNB1 mRNA expression was determined by RT-qPCR following KPNB1 overexpression or knockdown in HUCCT1 cells.(B) Representative images and quantitative analysis of colony formation assays following KPNB1 overexpression or knockdown.(C) Cell proliferation was assessed using CCK-8 assays following KPNB1 overexpression or knockdown.(D) The mRNA expression of stemness-related genes was determined by RT-qPCR following KPNB1 overexpression or knockdown.(E) Representative images and quantitative analysis of Transwell migration and invasion assays (10×).(F) Representative images and quantitative analysis of wound-healing assays at 0 and 48 h (4×).(G–H) Representative fluorescence images of F-actin staining following KPNB1 overexpression (G) or knockdown (H) (40×). (I–J) Representative Western blot images and quantitative analysis of EMT- and stemness-associated proteins following KPNB1 overexpression (I) or knockdown (J). GAPDH was used as the loading control.Each experiment was performed in triplicate. Quantitative data are presented as mean ± SD. **P* < 0.05, ***P* < 0.01, ****P* < 0.001, compared with the corresponding vector or control group. DAPI, 4′,6-diamidino-2-phenylindole; EMT, epithelial–mesenchymal transition; mRNA, messenger RNA; RT-qPCR, reverse transcription quantitative polymerase chain reaction; SD, standard deviation; siKPNB1, small interfering RNA targeting KPNB1; KD, kilodaltons.

 DOI: 10.14218/JCTH.2026.00370 | 2026

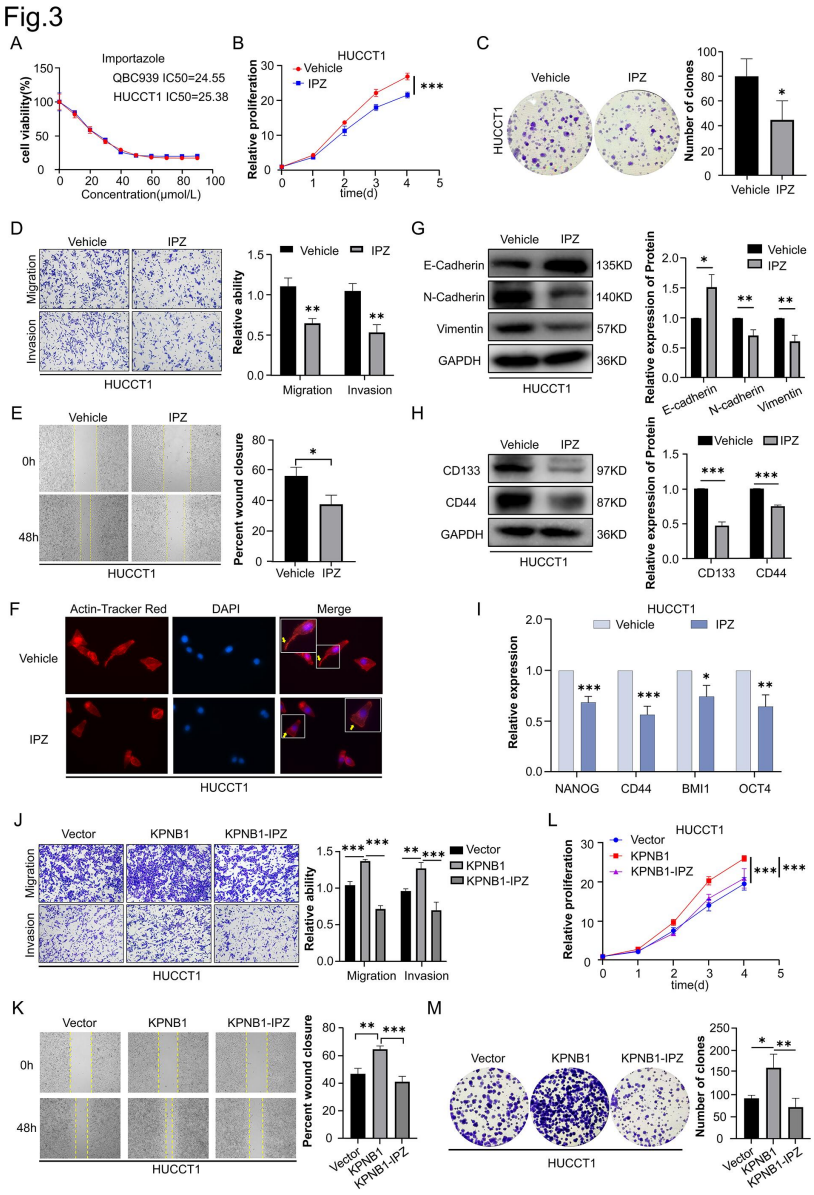


Fig. 3. Effects of pharmacological KPNB1 inhibition on cholangiocarcinoma cells. (A) Cell viability was assessed using CCK-8 assays in HUCCT1 and QBC939 cells treated with different concentrations of importazole (IPZ), and IC_{50} values were calculated from the dose–response curves. (B) Cell proliferation was assessed using CCK-8 assays following IPZ treatment. (C) Representative images and quantitative analysis of colony formation assays following IPZ treatment. (D–E) Representative images and quantitative analysis of Transwell migration and invasion assays (D, 10×) and wound-healing assays (E, 4×) following IPZ treatment. Wound closure was evaluated at 0 and 48 h. (F) Representative fluorescence images of F-actin staining following IPZ treatment (40×). (G–H) Representative Western blot images and quantitative analysis of EMT-associated proteins (G) and stemness-associated proteins (H) following IPZ treatment. GAPDH was used as the loading control. (I) The mRNA expression of stemness-related genes was determined by RT-qPCR following IPZ treatment. (J–M) The effects of IPZ treatment on KPNB1-overexpression-induced malignant phenotypes were evaluated in HUCCT1 cells. Representative images and quantitative analysis of Transwell migration and invasion assays (J, 10×), wound-healing assays (K, 4×), CCK-8 proliferation assays (L), and colony formation assays (M) are shown. Each experiment was performed in triplicate. Quantitative data are presented as mean ± SD. *$P < 0.05$, **$P < 0.01$, ***$P < 0.001$. DAPI, 4′,6-diamidino-2-phenylindole; EMT, epithelial–mesenchymal transition; IC_{50}, half-maximal inhibitory concentration; IPZ, importazole; mRNA, messenger RNA; RT-qPCR, reverse transcription quantitative polymerase chain reaction; SD, standard deviation; KD, kilodaltons.

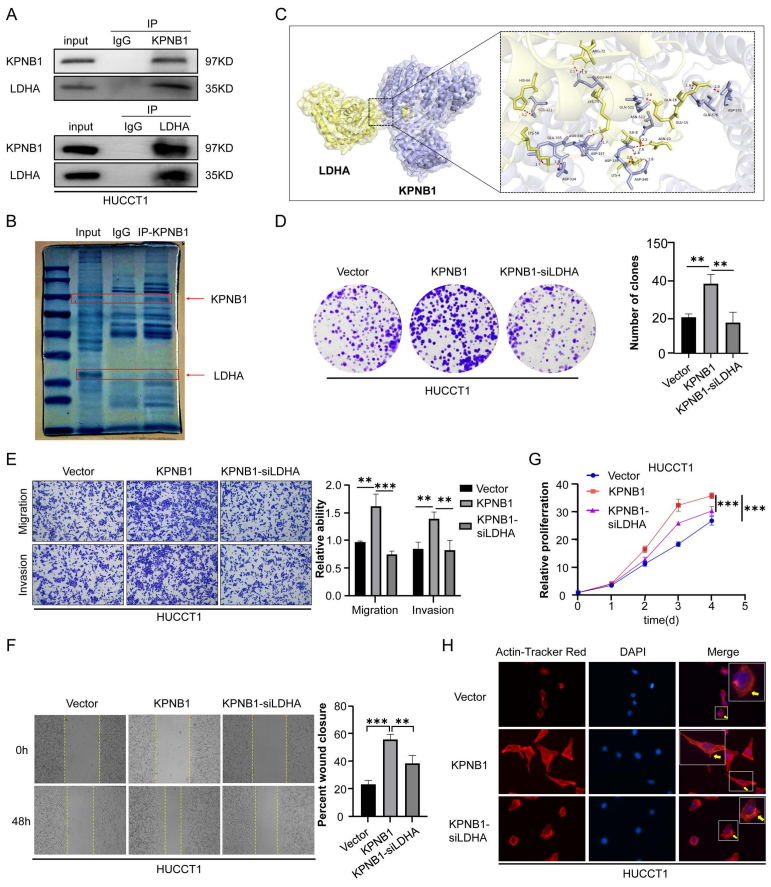


Fig. 4. Interaction of KPNB1 with LDHA and functional effects. (A) Reciprocal co-immunoprecipitation (Co-IP) assays showing the interaction between endogenous KPNB1 and LDHA in HUCCT1 cells. IgG was used as the negative control. (B) Coomassie Brilliant Blue staining of proteins immunoprecipitated with KPNB1. The positions of KPNB1 and LDHA are indicated. (C) Molecular docking analysis showing the predicted interaction between KPNB1 and LDHA. (D) Representative images and quantitative analysis of colony formation assays. (E–F) Representative images and quantitative analysis of Transwell migration and invasion assays (E, 10×) and wound-healing assays (F, 4×). (G) Cell proliferation was assessed using CCK-8 assays. (H) Representative fluorescence images of F-actin staining (40×). Each experiment was performed in triplicate. Quantitative data are presented as mean ± SD. $^{**}P < 0.01$, $^{***}P < 0.001$. Co-IP, co-immunoprecipitation; DAPI, 4′,6-diamidino-2-phenylindole; IgG, immunoglobulin G; IP, immunoprecipitation; SD, standard deviation; siLDHA, small interfering RNA targeting LDHA.

findings, IPZ treatment reduced the nuclear accumulation of LDHA (Fig. 5D, Supplementary Fig. 5D).

Given the well-established oncogenic role of LDHA in tumorigenesis and cancer progression,[32,33] we next performed rescue experiments to determine whether the tumor-promoting effects of KPNB1 are mediated by promoting the nuclear accumulation of LDHA. LDHA overexpression enhanced the transcription of stemness-related genes (Supplementary Fig. 5E), whereas KPNB1 knockdown attenuated this effect (Fig. 5J, Supplementary Fig. 5F). CCK-8 and colony formation assays showed that KPNB1 knockdown significantly attenuated LDHA-induced cell proliferation (Fig. 5E and I; Supplementary Fig. 5G and J). Similarly, Transwell and wound-healing assays showed that KPNB1 knockdown significantly reduced LDHA-induced cell migration (Fig. 5F–G and Supplementary Fig. 5H–I). F-actin staining further confirmed reduced cytoskeletal remodeling following KPNB1 knockdown (Fig. 5H; Supplementary Fig. 5K). Collectively, these findings demonstrate that the tumor-promoting effects of KPNB1 are mediated, at least in part, by promoting the nuclear accumulation of LDHA.

Nuclear LDHA cooperates with SOX2 to regulate stemness-associated phenotypes

Bioinformatic analysis predicted SOX2 as a potential transcription factor interacting with LDHA and implicated this interaction in malignant tumor progression.[34] To validate this prediction, Co-immunoprecipitation assays were performed using nuclear extracts from CCA cells. The results demonstrated that LDHA physically interacted with SOX2 in the nucleus (Fig. 6A, Supplementary Fig. 6A). To determine whether the LDHA-SOX2 interaction has functional consequences for transcriptional

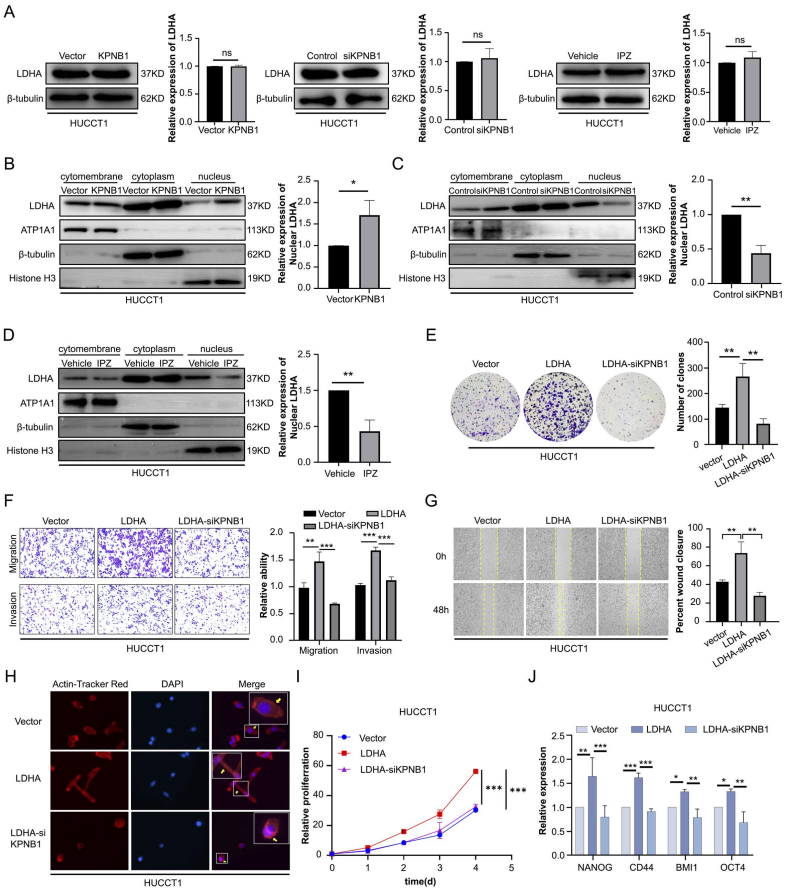


Fig. 5. KPNB1-mediated nuclear accumulation of LDHA. (A) Total LDHA protein levels were detected by Western blot analysis following KPNB1 overexpression, KPNB1 knockdown, or importazole (IPZ) treatment. Representative Western blot images and quantitative analyses are shown, with β-tubulin used as the loading control. (B–D) LDHA protein distribution in membrane, cytoplasmic, and nuclear fractions was examined by subcellular fractionation followed by Western blot analysis after KPNB1 overexpression (B), KPNB1 knockdown (C), or IPZ treatment (D). Quantitative analyses of nuclear LDHA expression are shown. ATP1A1, β-tubulin, and histone H3 were used as membrane, cytoplasmic, and nuclear markers, respectively. (E) Representative images and quantitative analysis of colony formation assays. (F–G) Representative images and quantitative analysis of Transwell migration and invasion assays (F, 10×) and wound-healing assays (G, 4×). (H) Representative fluorescence images of F-actin staining (40×). (I) Cell proliferation was assessed using CCK-8 assays. (J) The mRNA expression of stemness-related genes was determined by RT-qPCR. Each experiment was performed in triplicate. Quantitative data are presented as mean ± SD. ns, not statistically significant; **P* < 0.05, ***P* < 0.01, ****P* < 0.001. DAPI, 4′,6-diamidino-2-phenylindole; IPZ, importazole; mRNA, messenger RNA; RT-qPCR, reverse transcription quantitative polymerase chain reaction; SD, standard deviation; siRNA, small interfering RNA; KD, kilodaltons.

regulation, we performed dual-luciferase reporter assays using a NANOG promoter reporter (Fig. 6B). Consistent with previous findings,[35] SOX2 significantly increased NANOG promoter activity compared with the vector control (Fig. 6C, Supplementary Fig. 6B), confirming the responsiveness of the reporter to SOX2. Furthermore, SOX2 knockdown markedly attenuated the LDHA-associated increase in NANOG promoter activity (Fig. 6D, Supplementary Fig. 6C), suggesting that SOX2 is required for the transcriptional activation observed in LDHA-overexpressing cells.

Consistent with the dual-luciferase reporter results, SOX2 knockdown significantly attenuated the LDHA-induced upregulation of stemness-associated genes (Fig. 6E, Supplementary Fig. 6D). Western blot analysis showed that SOX2 knockdown effectively reduced LDHA-mediated upregulation of the stemness markers CD133 and CD44 (Fig. 6F, Supplementary Fig. 6E). Functionally, SOX2 deficiency significantly attenuated LDHA-induced cell proliferation (Fig. 6G–H, Supplementary Fig. 6I–J) and reduced LDHA-induced cell migration and invasion (Fig. 6J–K; Supplementary Fig. 6F–G). F-actin staining further demonstrated reduced cytoskeletal remodeling following SOX2 knockdown (Fig. 6I, Supplementary Fig. 6H). These findings suggest that nuclear LDHA promotes stemness-associated malignant phenotypes, at

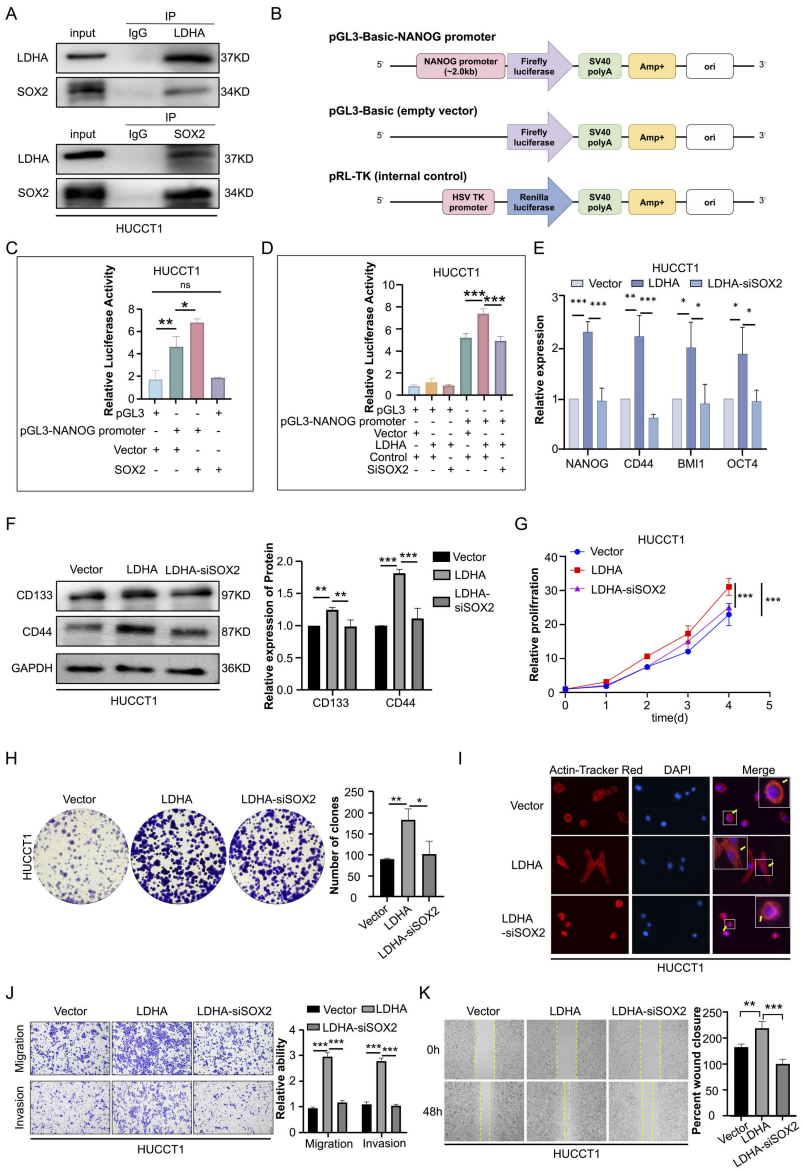


Fig. 6. Interaction between nuclear LDHA and SOX2 in cholangiocarcinoma cells. (A) Reciprocal co-immunoprecipitation (Co-IP) assays showing the interaction between LDHA and SOX2 in nuclear extracts from HUCCT1 cells. IgG was used as the negative control. (B) Schematic diagrams of the plasmids used for the dual-luciferase reporter assay, including the NANOG promoter-driven firefly luciferase reporter (pGL3-Basic-NANOG promoter), the promoterless pGL3-Basic vector, and the Renilla luciferase internal control plasmid (pRL-TK). (C) Dual-luciferase reporter assays showing the effects of SOX2 overexpression on NANOG promoter activity in HUCCT1 cells. (D) Dual-luciferase reporter assays. Firefly luciferase activity was normalized to Renilla luciferase activity. (E) The mRNA expression of stemness-related genes was determined by RT-qPCR. (F) Representative Western blot images and quantitative analysis of stemness-associated proteins. GAPDH was used as the loading control. (G) Cell proliferation was assessed using CCK-8 assays. (H) Representative images and quantitative analysis of colony formation assays. (I) Representative fluorescence images of F-actin staining (40×). (J–K) Representative images and quantitative analysis of Transwell migration and invasion assays (J, 10×) and wound-healing assays (K, 4×). Each experiment was performed in triplicate. Quantitative data are presented as mean ± SD. **P* < 0.05, ***P* < 0.01, ****P* < 0.001; ns, not statistically significant. Amp^{+}, ampicillin-resistance marker; Co-IP, co-immunoprecipitation; DAPI, 4′,6-diamidino-2-phenylindole; HSV TK, herpes simplex virus thymidine kinase; IgG, immunoglobulin G; IP, immunoprecipitation; kb, kilobases; kD, kilodaltons; mRNA, messenger RNA; ori, origin of replication; polyA, polyadenylation signal; RT-qPCR, reverse transcription quantitative polymerase chain reaction; SD, standard deviation; siSOX2, small interfering RNA targeting SOX2; SV40, simian virus 40.

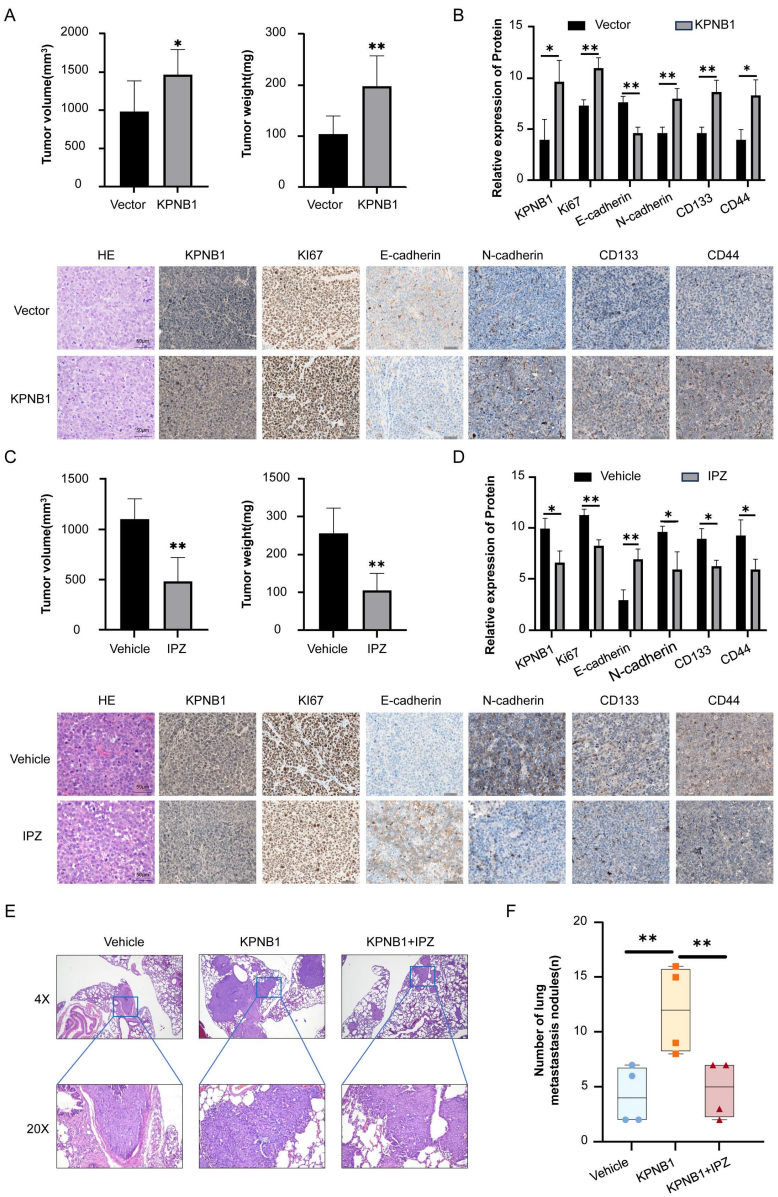


Fig. 7. Effects of KPNB1 on tumor growth and pulmonary metastasis *in vivo*. (A) Tumor volume and tumor weight of subcutaneous xenografts derived from HUCCT1 cells stably overexpressing KPNB1 or expressing the control vector (n = 6 mice/group). (B) Representative hematoxylin and eosin (H&E) staining and immunohistochemical staining for KPNB1, Ki-67, E-cadherin, N-cadherin, CD133, and CD44, together with quantitative analysis of immunohistochemical staining in xenograft tissues (40×). (C) Tumor volume and tumor weight of subcutaneous xenografts derived from parental HUCCT1 cells in mice treated with importazole (IPZ) or vehicle (n = 5 mice/group). (D) Representative H&E staining and immunohistochemical staining for KPNB1, Ki-67, E-cadherin, N-cadherin, CD133, and CD44, together with quantitative analysis of immunohistochemical staining in xenograft tissues following IPZ or vehicle treatment (40×). (E) Representative H&E-stained lung sections from the control, KPNB1-overexpression, and KPNB1-overexpression plus IPZ treatment groups in the experimental pulmonary metastasis model. The upper and lower panels show images at 4× and 20× magnification, respectively. (F) Quantification of pulmonary metastatic nodules in the experimental lung metastasis model (n = 4 mice/group). Data in (A–D) are presented as mean ± SD. Individual data points are shown in the box-and-whisker plots in (F). **P* < 0.05, ***P* < 0.01. H&E, hematoxylin and eosin; IPZ, importazole; SD, standard deviation.

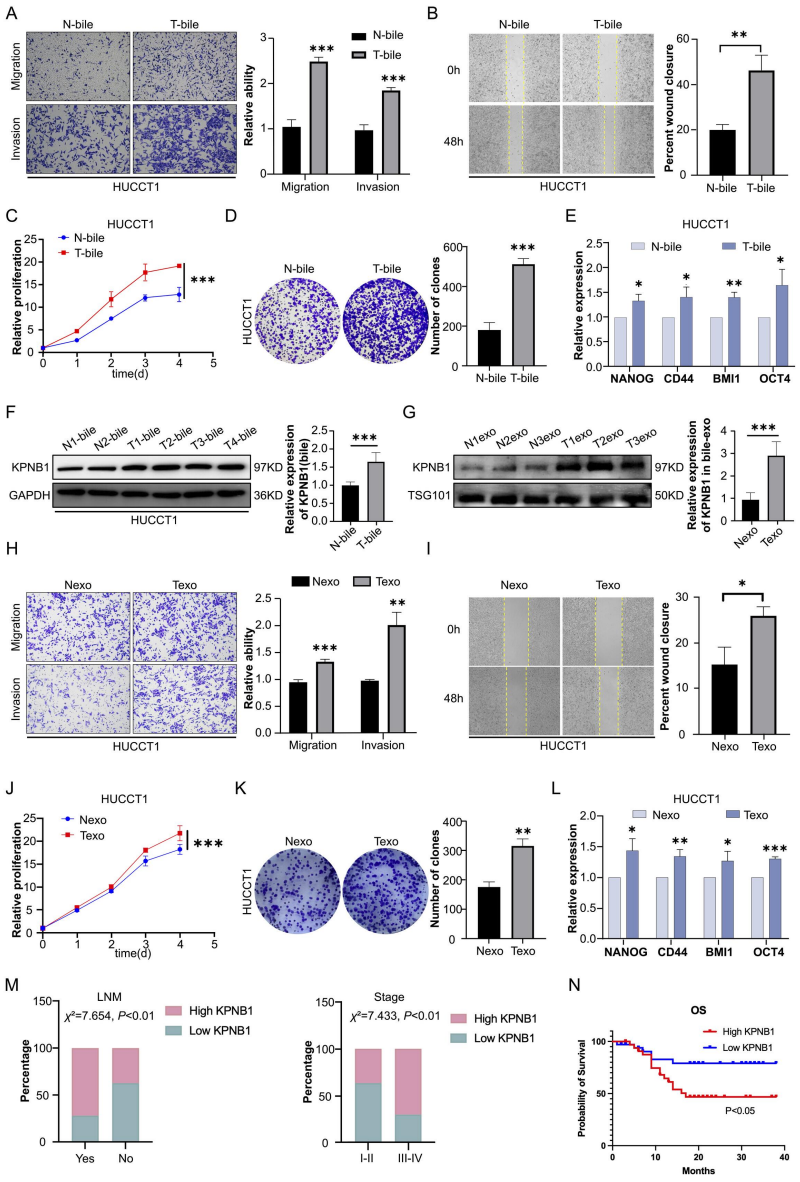


Fig. 8. Bile-associated KPNB1 expression and cholangiocarcinoma progression. (A) Representative images and quantitative analysis of Transwell migration and invasion assays (10×) in HUCCT1 cells treated with bile from non-tumor controls (N-bile) or patients with cholangiocarcinoma (T-bile). (B) Representative images and quantitative analysis of wound-healing assay (4×). (C) Cell viability was assessed by CCK-8 assay. (D) Colony formation assay. (E) mRNA expression of stemness-related genes was determined by RT-qPCR. (F) Western blot analysis of the effect of bile treatment on KPNB1 protein levels in HUCCT1 cells. GAPDH was used as the loading control. (G) KPNB1 protein levels in bile-derived exosomes were detected by Western blot assay. TSG101 was used as an exosomal marker. (H) Representative images and quantitative analysis of Transwell assays (10×) in HUCCT1 cells treated with exosomes isolated from non-tumor bile (Nexo) or cholangiocarcinoma bile (Texo). (I) Representative images and quantitative analysis of wound-healing assay (4×). (J) Cell viability was assessed by CCK-8 assay. (K) Colony formation assay. (L) mRNA expression of stemness-related genes was determined by RT-qPCR. (M) Correlation analysis between bile KPNB1 levels and clinicopathological characteristics, including lymph node metastasis and TNM stage. (N) Kaplan–Meier analysis of overall survival according to bile KPNB1 levels. The in vitro experiments were performed in triplicate. Quantitative data from the in vitro experiments are presented as mean ± SD. *P < 0.05, **P < 0.01, ***P < 0.001. eCCA, extrahepatic cholangiocarcinoma; LNM, lymph node metastasis; mRNA, messenger RNA; N-bile, non-tumor control bile; Nexo, non-tumor bile-derived exosomes; OS, overall survival; RT-qPCR, reverse transcription quantitative polymerase chain reaction; SD, standard deviation; T-bile, cholangiocarcinoma-derived bile; Texo, cholangiocarcinoma bile-derived exosomes; TNM, tumor–node–metastasis; TSG101, tumor susceptibility gene 101; KD, kilodaltons.

least in part, through its interaction with SOX2 and enhancement of *SOX2*-dependent transcription.

KPNB1 promotes tumor growth and pulmonary metastasis in vivo

To investigate the role of KPNB1 *in vivo*, subcutaneous xenograft and experimental pulmonary metastasis models were established using HUCCT1 cells. KPNB1 overexpression markedly promoted xenograft growth (Supplementary Fig. 7A), as evidenced by increased tumor volume and weight (Fig. 7A), together with elevated expression of Ki-67, N-cadherin, CD133, and CD44 and reduced E-cadherin expression (Fig. 7B). Conversely, pharmacological inhibition of KPNB1 with IPZ markedly suppressed tumor growth and reversed these molecular alterations (Fig. 7C–D, Supplementary Fig. 7B).

In the experimental pulmonary metastasis model, KPNB1 overexpression markedly increased the number of metastatic lung nodules, whereas IPZ treatment substantially reduced the pulmonary metastatic burden (Fig. 7E–F, Supplementary Fig. 7C). These results demonstrate that KPNB1 promotes cholangiocarcinoma growth and pulmonary metastasis *in vivo*, whereas pharmacological inhibition of KPNB1 effectively suppresses these malignant phenotypes.

Bile-derived KPNB1 is associated with cholangiocarcinoma progression and poor clinical outcome

Having established the oncogenic role of the KPNB1–LDHA–SOX2 axis, we next sought to identify the upstream microenvironmental signals associated with KPNB1 upregulation. Accordingly, HUCCT1 and QBC939 cells were treated with bile samples obtained from patients with eCCA or non-tumor controls. Compared with control bile, eCCA-derived bile markedly enhanced cell proliferation, migration, and invasion (Fig. 8A–D; Supplementary Fig. 7D–G). Consistently, F-actin staining demonstrated increased cytoskeletal remodeling and pseudopodia formation (Supplementary Fig. 7I–J), accompanied by increased expression of stemness-related genes (Fig. 8E, Supplementary Fig. 7H).

To determine whether KPNB1 mediates the biological effects of bile, KPNB1 expression was examined following bile treatment. Western blot analysis showed that eCCA-derived bile markedly increased KPNB1 protein expression (Fig. 8F, Supplementary Fig. 7K), whereas *KPNB1* mRNA levels remained unchanged (Supplementary Fig. 7L). Importantly, KPNB1 knockdown significantly attenuated bile-induced cell proliferation and migration in CCA cells (Supplementary Fig. 8A–F). Likewise, pharmacological inhibition of KPNB1 with IPZ significantly reversed the malignant phenotypes induced by eCCA-derived bile (Supplementary Fig. 9A–F), indicating that KPNB1 contributes to the tumor-promoting effects of eCCA-derived bile.

Given that eCCA-derived bile increased KPNB1 protein without altering *KPNB1* mRNA expression, we next investigated whether bile-derived exosomes contribute to this effect. Exosomes were successfully isolated and characterized by transmission electron microscopy (Supplementary Fig. 10A), NanoFCM-based particle size analysis (Supplementary Fig. 10B), and Western blot analysis (Supplementary Fig. 10C). PKH67 labeling demonstrated efficient uptake of bile-derived exosomes by CCA cells (Supplementary Fig. 10I). Notably, exosomes isolated from eCCA bile contained higher levels of KPNB1 than those isolated from non-tumor bile (Fig. 8G) and markedly promoted CCA cell proliferation, migration, and stemness (Fig. 8H–L, Supplementary Fig. 10D–H), closely recapitulating the biological effects of whole bile. These findings suggest that bile-derived exosomes may contribute to the tumor-promoting activity of the biliary microenvironment, potentially through the delivery of KPNB1 to CCA cells.

Finally, to assess the clinical applicability of bile-derived KPNB1, KPNB1 levels were quantified by ELISA in bile samples from 70 patients with eCCA. Elevated bile KPNB1 levels were significantly associated with lymph node metastasis and advanced TNM stage (Fig. 8M). Kaplan–Meier survival analysis further showed that patients with high bile KPNB1 levels had significantly shorter overall survival than those with low KPNB1 levels (Fig. 8N). ROC curve analysis demonstrated that bile KPNB1 had the highest AUC among the four evaluated biomarkers, followed by CA19-9, AFP, and CEA (Supplementary Fig. 10J–K). Collectively, these findings demonstrate that elevated bile KPNB1 levels are associated with aggressive disease characteristics and suggest that bile KPNB1 may have potential clinical value for postoperative risk stratification.

Discussion

In this study, we identified KPNB1 as a potential driver of CCA progression, with elevated KPNB1 expression associated with aggressive clinicopathological features and poor clinical outcomes. Functional analyses demonstrated that KPNB1 promotes CCA cell proliferation, migration, and stemness, as well as tumor growth and pulmonary metastasis *in vivo*. Mechanistically, KPNB1 facilitates the nuclear accumulation of LDHA, enabling its interaction with SOX2 and enhancing stemness-associated transcription. Furthermore, eCCA-derived bile promoted KPNB1 protein accumulation, with bile-derived exosomes emerging as a potential upstream mediator. Elevated bile KPNB1 levels were also associated with adverse clinical outcomes. Collectively, these findings identify the KPNB1–LDHA–SOX2 axis as a potential mechanistic link between the biliary microenvironment and CCA progression.

Aberrant nucleocytoplasmic transport is increasingly recognized as a hallmark of tumor progression and is characterized by the dysregulated subcellular localization of key regulatory proteins.[36,37] As a central receptor in the classical nuclear import pathway, KPNB1 is highly expressed across multiple malignancies and promotes tumor progression by facilitating the nuclear transport of oncogenic proteins.[14] Previous studies have implicated KPNB1 in the malignant progression of acute myeloid leukemia,[38] hepatocellular carcinoma,[39] prostate cancer, and gastric cancer.[41] Consistent with these findings, our study demonstrated that KPNB1 is upregulated in CCA tissues and associated with poor clinical outcomes. Moreover, pharmacological inhibition of KPNB1 with IPZ attenuated malignant phenotypes both *in vitro* and *in vivo*, supporting KPNB1 as a potential therapeutic target for CCA.

To define the molecular basis of KPNB1-driven tumor progression, we next investigated its potential downstream interacting partners. KPNB1 promotes tumor progression across

multiple malignancies by facilitating the nuclear translocation of diverse oncogenic proteins. In glioblastoma, KPNB1 mediates the nuclear translocation of YBX1, thereby promoting tumor progression.[23] In non-small cell lung cancer, KPNB1 promotes the nuclear translocation of PD-L1, contributing to tumor cell proliferation and radioresistance.[22,42] Similarly, KPNB1 inhibition suppresses cervical cancer cell growth by impairing NF-κB nuclear import.[24] Consistent with these findings, we identified LDHA as a KPNB1-interacting protein in CCA cells. Notably, KPNB1 did not alter total LDHA protein expression but instead promoted its nuclear accumulation, indicating that the oncogenic function of LDHA may depend more on its subcellular localization than on its overall abundance.

LDHA is a key glycolytic enzyme that catalyzes the terminal step of anaerobic glucose metabolism.[43] In cancer, LDHA has traditionally been viewed as a metabolic driver of tumor progression through glycolytic reprogramming.[33,44,45] For example, in hepatocellular carcinoma, LDHA promotes tumor progression through YAP activation by inducing its dephosphorylation.[46] LDHA expression has also been associated with breast cancer prognosis, chemotherapeutic response, and immune infiltration.[47] However, accumulating evidence indicates that LDHA also exerts non-metabolic functions. Nuclear LDHA can act as a non-canonical enzyme by forming a transcriptional complex with HIF-1α, thereby promoting glycolysis in hepatic stellate cells and contributing to liver fibrosis.[48] In our study, we found that nuclear LDHA interacts with SOX2 and that the LDHA-SOX2 axis contributes to the maintenance of stemness and malignant progression in CCA.

SOX2, a pivotal transcription factor of the SOX family, sustains stem cell-like properties by regulating genes involved in self-renewal and cellular plasticity.[34] Dysregulated SOX2 expression has been reported in several solid tumors, including colorectal and pancreatic cancers, where it is associated with aggressive phenotypes and poor clinical outcomes. Accumulating evidence indicates that aberrant SOX2 activation promotes malignant progression through diverse mechanisms, including maintenance of stemness, induction of epithelial–mesenchymal transition (EMT), metabolic adaptation, and remodeling of the tumor microenvironment.[49,50] In our study, SOX2 suppression markedly attenuated LDHA-induced NANOG promoter activation and reduced the expression of stemness-associated genes, supporting a role for the LDHA–SOX2 interaction in regulating stemness-associated transcriptional activity in CCA cells.

The biliary microenvironment is increasingly recognized as a defining feature of CCA and a potential determinant of tumor progression. Bile components can establish a pro-tumorigenic niche and facilitate metastatic progression.[3] Multi-omics analyses have revealed distinct microbial and metabolic features of CCA bile,[51] while overlapping bacterial profiles between bile and tumor tissues, particularly those involving *Enterococcus* and *Staphylococcus aureus*, suggest potential microbial translocation. Notably, *S. aureus* has been identified as a potential species-level biomarker for CCA diagnosis and staging.[7] Bile components are also closely associated with biliary tumor initiation and progression and may provide clinically relevant biomarkers.[5] Consistent with these observations, eCCA-derived bile promoted malignant phenotypes and increased KPNB1 protein expression in CCA cells. Elevated bile KPNB1 levels were further associated with adverse clinicopathological features and poor prognosis, supporting their potential utility for prognostic assessment in CCA.

Emerging evidence indicates that extracellular vesicles, particularly exosomes, mediate intercellular communication within the tumor microenvironment by delivering proteins, nucleic acids, and metabolites to recipient cells, thereby altering their functional state.[52-54] In our study, eCCA-derived bile increased intracellular KPNB1 protein abundance without affecting *KPNB1* mRNA levels. Notably, KPNB1 was enriched in bile-derived exosomes from patients with eCCA, which largely recapitulated the pro-tumorigenic effects of whole bile. Together, these findings suggest that bile-derived exosomes may contribute, at least in part, to the tumor-promoting effects of the biliary microenvironment.

Despite these findings, several limitations warrant consideration. First, although our data support a role for KPNB1 in promoting the nuclear accumulation of LDHA, they do not establish LDHA as a direct KPNB1 cargo. Whether LDHA contains a functional nuclear localization signal or requires adaptor proteins for KPNB1-mediated nuclear import remains to be determined. Second, although our findings support functional cooperation between *LDHA* and *SOX2* in transcriptional regulation, chromatin immunoprecipitation (ChIP)-based studies are needed to determine whether nuclear LDHA directly affects SOX2 occupancy at target gene promoters. Third, although bile-derived exosomes were enriched in KPNB1 and largely recapitulated the biological effects of whole bile, the direct contribution of exosomal KPNB1 to these effects and its clinical utility remain to be established.

Conclusions

In summary, this study identifies KPNB1 as a potential driver of cholangiocarcinoma progression by promoting the nuclear accumulation of LDHA and subsequent *SOX2*-dependent transcription. Pharmacological inhibition of KPNB1 suppresses malignant phenotypes *in vitro* and *in vivo*, supporting its potential as a therapeutic target. Furthermore, eCCA-derived bile promotes KPNB1 protein accumulation, while elevated bile KPNB1 levels are associated with adverse clinical outcomes, supporting its potential value for prognostic assessment. Collectively, these findings implicate the KPNB1–LDHA–SOX2 axis as a potential molecular link between the biliary microenvironment and cholangiocarcinoma progression.

Supporting information

Supplementary material for this article is available at https://doi.org/10.14218/JCTH.2026.00370.

Acknowledgments

We gratefully acknowledge all participants of this study for their contributions.

Funding

The Natural Science Foundation Innovation and Development

Joint Fund of Shandong Province (grant number ZR2024LZL014), the Jointly-built Science and Technology Project of the Science and Technology Department of the National Administration of Traditional Chinese Medicine (grant number GZY-KJS-SD-2023-075), Shandong Provincial Key Research and Development Program (Competitive Innovation Platform) (grant number 2025CXPT132), the National Natural Science Foundation of China (grant number 82370890), Taishan Scholars Program of Shandong Province (grant number tsqn202312382), the National Natural Science Foundation of Shandong Province (grant number ZR2023MH243).

Conflict of interest

The authors have no conflict of interest related to this publication.

Author contributions

Study concept and design (FD, XZ, YX), acquisition of data (FD, XZ), analysis and interpretation of data (FD, HZ, KLi, KLiu), drafting of the manuscript (FD, CZ), critical revision of the manuscript for important intellectual content (CZ, BD, PG), administrative, technical, or material support (CZ, BD), and study supervision (CZ). All authors have made a significant contributions to this study and have approved the final manuscript.

Ethical statement

The study was approved by the Institutional Ethics Committee of The Affiliated Hospital of Qingdao University (Approval No. QYFYWZLL30901). Written informed consent was obtained from all participants. The study was conducted in accordance with the Declaration of Helsinki (as revised in 2024). All animal procedures were approved by the Animal Ethics Committee of The Affiliated Hospital of Qingdao University (No. AHQU-MAL20250609DFQ) and conducted in accordance with the Chinese national standard Laboratory animals—General code of animal welfare (GB/T 42011–2022). All animals received humane care. For the subcutaneous xenograft experiments, the approved humane endpoints were a maximum tumor diameter of 20 mm or a tumor volume of 2,000 mm^3, whichever occurred first.

Data sharing statement

The mass spectrometry proteomics data have been deposited with the ProteomeXchange Consortium via the iProX partner repository with the dataset identifier PXD082460. All other data supporting the findings of this study are available from the corresponding author upon reasonable request.

References

[1] Banales JM, Marin JJG, Lamarca A, Rodrigues PM, Khan SA, Roberts LR, *et al*. Cholangiocarcinoma 2020: the next horizon in mechanisms and management. Nat Rev Gastroenterol Hepatol 2020;17(9):557–588. DOI: 10.1038/s41575-020-0310-z, PMID: 32606456.

[2] Macarulla T, Neuzillet C, Prager GW, Rimassa L, Bridgewater J. Opportunities and Approaches to Optimising Advanced Cholangiocarcinoma Outcomes in the Era of Targeted Therapies: A Narrative Review. Oncol Ther 2025;13(4):939–962. DOI: 10.1007/s40487-025-00370-2, PMID: 41060610.

[3] Gao R, Wei B, Li K, Zou H, Cao J, Dong Q, *et al*. Metastatic microenvironment of extrahepatic cholangiocarcinoma. Int J Surg 2026;112(2):4452–4466. DOI: 10.1097/JS9.0000000000003852, PMID: 41202326.

[4] Wu T, Gao R, Wang X, Guo D, Xie Y, Dong B, *et al*. Pancreatobiliary reflux increases macrophage-secreted IL-8 and activates the PI3K/NFκB pathway to promote cholangiocarcinoma progression. Transl Oncol 2024;45:101967. DOI: 10.1016/j.tranon.2024.101967, PMID: 38653100.

[5] Li YC, Li KS, Liu ZL, Tang YC, Hu XQ, Li XY, *et al*. Research progress of bile biomarkers and their immunoregulatory role in biliary tract cancers. Front Immunol 2022;13:1049812. DOI: 10.3389/fimmu.2022.1049812, PMID: 36389727.

[6] Huang F, Liu Z, Song Y, Wang G, Shi A, Chen T, *et al*. Bile acids activate cancer-associated fibroblasts and induce an immunosuppressive microenvironment in cholangiocarcinoma. Cancer Cell 2025;43(8):1460–1475.e10. DOI: 10.1016/j.ccell.2025.05.017, PMID: 40578361.

[7] Wang L, Zhao H, Wu F, Chen J, Xu H, Gong W, *et al*. Bile-Liver phenotype: Exploring the microbiota landscape in bile and intratumor of cholangiocarcinoma. Comput Struct Biotechnol J 2025;27:1173–1186. DOI: 10.1016/j.csbj.2025.03.030, PMID: 40206347.

[8] Zhuo Z, Xie Y, Zou H, Tan B, Dong Q, Dong B, *et al*. Review: Progress of the NLRP3 inflammasome in tumours and perspectives for cholangiocarcinoma. Cell Commun Signal 2025;23(1):405. DOI: 10.1186/s12964-025-02416-4, PMID: 41035012.

[9] Louis C, Desoteux M, Coulouarn C. Exosomal circRNAs: new players in the field of cholangiocarcinoma. Clin Sci (Lond) 2019;133(21):2239–2244. DOI: 10.1042/CS20190940, PMID: 31654054.

[10] Ikeda C, Haga H, Makino N, Inuzuka T, Kurimoto A, Ueda T, *et al*. Utility of Claudin-3 in extracellular vesicles from human bile as biomarkers of cholangiocarcinoma. Sci Rep 2021;11(1):1195. DOI: 10.1038/s41598-021-81023-y, PMID: 33441949.

[11] Yoshida M, Yukawa H, Hayashi K, Naitoh I, Miyabe K, Hori Y, *et al*. Clinical impact of bile-derived exosomal microRNAs as novel diagnostic and prognostic biomarkers for biliary tract cancers. Cancer Sci 2023;114(1):295–305. DOI: 10.1111/cas.15597, PMID: 36168845.

[12] Pan Y, Shao S, Sun H, Zhu H, Fang H. Bile-derived exosome noncoding RNAs as potential diagnostic and prognostic biomarkers for cholangiocarcinoma. Front Oncol 2022;12:985089. DOI: 10.3389/fonc.2022.985089, PMID: 36091129.

[13] Zheng Y, Yu K, Lin JF, Liang Z, Zhang Q, Li J, *et al*. Deep learning prioritizes cancer mutations that alter protein nucleocytoplasmic shuttling to drive tumorigenesis. Nat Commun 2025;16(1):2511. DOI: 10.1038/s41467-025-57858-8, PMID: 40087285.

[14] Shi Q, Lin M, Cheng X, Zhang Z, Deng S, Lang K, *et al*. KPNB1-mediated nuclear import in cancer. Eur J Pharmacol 2023;955:175925. DOI: 10.1016/j.ejphar.2023.175925, PMID: 37473981.

[15] Wing CE, Chook YM. Multiple roads between the nucleus and the cytoplasm: classes of linear NLSs and NESs and their receptors. Curr Opin Struct Biol 2026;98:103244. DOI: 10.1016/j.sbi.2026.103244, PMID: 41825110.

[16] Wang T, Huang Z, Huang N, Peng Y, Gao M, Wang X, *et al*. Inhibition of KPNB1 Inhibits Proliferation and Promotes Apoptosis of Chronic Myeloid Leukemia Cells Through Regulation of E2F1. Onco Targets

Ther 2019;12:10455–10467. DOI: 10.2147/OTT.S210048, PMID: 31819526.

[17] Lombardi Z, Gardini L, Kashchuk AV, Menconi A, Lulli M, Tusa I, *et al*. Importin subunit beta-1 mediates ERK5 nuclear translocation, and its inhibition synergizes with ERK5 kinase inhibitors in reducing cancer cell proliferation. Mol Oncol 2025;19(1):99–113. DOI: 10.1002/1878-0261.13674, PMID: 38965815.

[18] Zhang Y, Li KF. Karyopherin β1 deletion suppresses tumor growth and metastasis in colorectal cancer (CRC) by reducing MET expression. Biomed Pharmacother 2019;120:109127. DOI: 10.1016/j.biopha.2019.109127, PMID: 31629952.

[19] Park C, Oh J, Lee WM, Koh HR, Sohn UD, Ham SW, *et al*. Inhibition of NUPR1-Karyopherin β1 Binding Increases Anticancer Drug Sensitivity. Int J Mol Sci 2021;22(6):2794. DOI: 10.3390/ijms22062794, PMID: 33801927.

[20] van der Watt PJ, Maske CP, Hendricks DT, Parker MI, Denny L, Govender D, *et al*. The Karyopherin proteins, Crm1 and Karyopherin beta1, are overexpressed in cervical cancer and are critical for cancer cell survival and proliferation. Int J Cancer 2009;124(8):1829–1840. DOI: 10.1002/ijc.24146, PMID: 19117056.

[21] Yang J, Guo Y, Lu C, Zhang R, Wang Y, Luo L, *et al*. Inhibition of Karyopherin beta 1 suppresses prostate cancer growth. Oncogene 2019;38(24):4700–4714. DOI: 10.1038/s41388-019-0745-2, PMID: 30742095.

[22] Du W, Zhu J, Zeng Y, Liu T, Zhang Y, Cai T, *et al*. KPNB1-mediated nuclear translocation of PD-L1 promotes non-small cell lung cancer cell proliferation via the Gas6/MerTK signaling pathway. Cell Death Differ 2021;28(4):1284–1300. DOI: 10.1038/s41418-020-00651-5, PMID: 33139930.

[23] Li J, Zhang B, Feng Z, An D, Zhou Z, Wan C, *et al*. Stabilization of KPNB1 by deubiquitinase USP7 promotes glioblastoma progression through the YBX1-NLGN3 axis. J Exp Clin Cancer Res 2024;43(1):28. DOI: 10.1186/s13046-024-02954-8, PMID: 38254206.

[24] Chi RA, van der Watt P, Wei W, Birrer MJ, Leaner VD. Inhibition of Kpnβ1 mediated nuclear import enhances cisplatin chemosensitivity in cervical cancer. BMC Cancer 2021;21(1):106. DOI: 10.1186/s12885-021-07819-3, PMID: 33530952.

[25] Soderholm JF, Bird SL, Kalab P, Sampathkumar Y, Hasegawa K, Uehara-Bingen M, *et al*. Importazole, a small molecule inhibitor of the transport receptor importin-β. ACS Chem Biol 2011;6(7):700–708. DOI: 10.1021/cb2000296, PMID: 21469738.

[26] Yuwei X, Bingzi D, Zhaowei S, Yujie F, Wei Z, Kun L, *et al*. FEN1 promotes cancer progression of cholangiocarcinoma by regulating the Wnt/β-catenin signaling pathway. Dig Liver Dis 2024;56(4):695–704. DOI: 10.1016/j.dld.2023.08.050, PMID: 37648642.

[27] Jin C, Dong B, Xie Y, Chen X, Wu S, Du F, *et al*. LncRNA938/ TAF9/TTK axis promotes EMT and serves as a therapeutic target in hepatoblastoma. J Transl Med 2025;23(1):946. DOI: 10.1186/s12967-025-06809-4, PMID: 40841910.

[28] He T, Zhang Q, Xu P, Tao W, Lin F, Liu R, *et al*. Extracellular vesicle-circEHD2 promotes the progression of renal cell carcinoma by activating cancer-associated fibroblasts. Mol Cancer 2023;22(1):117. DOI: 10.1186/s12943-023-01824-9, PMID: 37481520.

[29] Liu Y, Shi M, He X, Cao Y, Liu P, Li F, *et al*. LncRNA-PACERR induces pro-tumour macrophages via interacting with miR-671-3p and m6A-reader IGF2BP2 in pancreatic ductal adenocarcinoma. J Hematol Oncol 2022;15(1):52. DOI: 10.1186/s13045-022-01272-w, PMID: 35526050.

[30] Shen Q, Han Y, Wu K, He Y, Jiang X, Liu P, *et al*. MrgprF acts as a tumor suppressor in cutaneous melanoma by restraining PI3K/Akt signaling. Signal Transduct Target Ther 2022;7(1):147. DOI: 10.1038/s41392-022-00945-9, PMID: 35504869.

[31] Wang Y, Xie Y, Dong B, Xue W, Chen S, Mitsuo S, *et al*. The TTYH3/MK5 Positive Feedback Loop regulates Tumor Progression via GSK3-β/β-catenin signaling in HCC. Int J Biol Sci 2022;18(10):4053–4070. DOI: 10.7150/ijbs.73009, PMID: 35844789.

[32] Lu RS, Ren LK, Fei XB, Liu SB, Gao YJ, Hou JY, *et al*. PSMD14-Mediated LDHA Deubiquitination Upregulates ACLY Expression via H3K18 Lactylation to Promote Lipid Synthesis and Pancreatic Cancer Progression. Adv Sci (Weinh) 2025;12(44):e05762. DOI: 10.1002/advs.202505762, PMID: 41051446.

[33] Feng Y, Xiong Y, Qiao T, Li X, Jia L, Han Y. Lactate dehydrogenase A: A key player in carcinogenesis and potential target in cancer therapy. Cancer Med 2018;7(12):6124–6136. DOI: 10.1002/cam4.1820, PMID: 30403008.

[34] Wang K, Li Y, Guo Z, Song L, Ding X, Liu L, *et al*. Role of the SOX family in non-small cell lung cancer: Molecular mechanisms and therapeutic implications (Review). Oncol Rep 2026;55(1):19. DOI: 10.3892/or.2025.9024, PMID: 41268614.

[35] Rodda DJ, Chew JL, Lim LH, Loh YH, Wang B, Ng HH, *et al*. Transcriptional regulation of nanog by OCT4 and SOX2. J Biol Chem 2005;280(26):24731–24737. DOI: 10.1074/jbc.M502573200, PMID: 15860457.

[36] Liu X, Wang W, Cao W, Li Z, Huang H, Liu F, *et al*. RAB3A-mediated BAG6 translocation promotes non-small cell lung cancer tumorigenesis and progression. Cell Oncol (Dordr) 2025;48(6):2001–2015. DOI: 10.1007/s13402-025-01123-z, PMID: 41123819.

[37] Zhou W, Qiu T, Wang J, Chen J, Jiang R, Teng Y, *et al*. Importin-7 facilitates cervical cancer progression through MSI2 nuclear import and is associated with MSI2-MYC-linked glycolytic reprogramming. Transl Res 2026;293:44–62. DOI: 10.1016/j.trsl.2026.04.007, PMID: 42066897.

[38] Xie Y, Zhao R, Zheng Y, Li Y, Wu F, Lei Y, *et al*. Targeting KPNB1 suppresses AML cells by inhibiting HMGB2 nuclear import. Oncogene 2025;44(21):1646–1661. DOI: 10.1038/s41388-025-03340-0, PMID: 40082556.

[39] Fang H, Shi X, Gao J, Yan Z, Wang Y, Chen Y, *et al*. TMEM209 promotes hepatocellular carcinoma progression by activating the Wnt/β-catenin signaling pathway through KPNB1 stabilization. Cell Death Discov 2024;10(1):438. DOI: 10.1038/s41420-024-02207-9, PMID: 39414762.

[40] Ma Q, Lu X, Tian W, Chen Y, He X. Astragaloside □ mediates the effect and mechanism of KPNB1 on biological behavior and tumor growth in prostate cancer. Heliyon 2024;10(13):e33904. DOI: 10.1016/j.heliyon.2024.e33904, PMID: 39027542.

[41] Zhang C, Wang X, Cai G, Wang H, Liu Q, Ma S, *et al*. Targeting KPNB1 with genkwadaphnin suppresses gastric cancer progression through the Nur77-mediated signaling pathway. Eur J Pharmacol 2024;977:176697. DOI: 10.1016/j.ejphar.2024.176697, PMID: 38823760.

[42] Zhu D, Lu M, Cheng H. NAT10 promotes radiotherapy resistance in non-small cell lung cancer by regulating KPNB1-mediated PD-L1 nuclear translocation. Open Life Sci 2025;20(1):20251065. DOI: 10.1515/biol-2025-1065, PMID: 40109769.

[43] He Q, Li H, Cong Y, Chen K, Cheng L, Lv F, *et al*. FAM111B enhances glycolysis and promotes metastasis of prostate cancer by upregulating LDHA. Neoplasia 2025;69:101227. DOI: 10.1016/j.neo.2025.101227, PMID: 40975977.

[44] Hou Y, Zhao Y, He Q, Wang M, Zhang Q. LDH isozymes as targets for

cancer therapy. J Enzyme Inhib Med Chem 2026;41(1):2639168. DOI: 10.1080/14756366.2026.2639168, PMID: 41837490.

[45] Stepanov YV, Solyanik GI, Yakshibaeva Y, Kolesnik D, Stepanova LI, Golovynska I. Suppression of Tumor Aggression Through Metabolic Reprogramming via Oxamate Targeting LDHA. Int J Mol Sci 2026; 27(7):3245. DOI: 10.3390/ijms27073245, PMID: 41977425.

[46] Wei X, Zou L, Huang Y, Qiu C, Cheng G, Chen Y, *et al*. LDHA-mediated YAP lactylation promotes the tumor progression of hepatocellular carcinoma by inducing YAP dephosphorylation and activation. Biol Direct 2025;20(1):64. DOI: 10.1186/s13062-025-00655-6, PMID: 40414964.

[47] Xia JQ, Wang YL, Li XL, Wang JN, Li FC, Jia SY, *et al*. Lactate dehydrogenase a is a crucial biomarker that affects the prognosis, chemotherapy effect, and immune infiltration of breast cancer. BMC Womens Health 2025;25(1):497. DOI: 10.1186/s12905-025-04039-w, PMID: 41107806.

[48] Wang F, Chen L, Kong D, Zhang X, Xia S, Liang B, *et al*. Canonical Wnt signaling promotes HSC glycolysis and liver fibrosis through an LDH-A/HIF-1α transcriptional complex. Hepatology 2024;79(3):606–623. DOI: 10.1097/HEP.0000000000000569, PMID: 37733267.

[49] Tang Q, Chen J, Di Z, Yuan W, Zhou Z, Liu Z, *et al*. TM4SF1 promotes EMT and cancer stemness via the Wnt/β-catenin/SOX2 pathway in colorectal cancer. J Exp Clin Cancer Res 2020;39(1):232. DOI: 10.1186/s13046-020-01690-z, PMID: 33153498.

[50] Zu F, Chen C, Geng Q, Li H, Chan B, Luo G, *et al*. Smad2 Cooperating with TGIF2 Contributes to EMT and Cancer Stem Cells Properties in Pancreatic Cancer via Co-Targeting SOX2. Int J Biol Sci 2025;21(2): 524–543. DOI: 10.7150/ijbs.102381, PMID: 39781447.

[51] Xia JY, Komanduri S, Keswani RN, Rodrigues TR, Sinha J, Rengarajan A, *et al*. Integrating multi-omics in bile for biomarker discovery in cholangiocarcinoma. Hepatol Commun 2025;9(9):e0786. DOI: 10.1097/HC9.0000000000000786, PMID: 40857390.

[52] Zhang J, Chen M. Exosomes and cholangiocarcinoma: mechanisms, diagnostic, and therapeutic perspectives. Front Immunol 2026;17: 1779516. DOI: 10.3389/fimmu.2026.1779516, PMID: 41939857.

[53] Wei X, Chen X, Ren Y, Tu M, Wu S, Guo T, *et al*. CAF-derived exosomal circMPP6 drives ovarian cancer metastasis by coordinating nuclear and cytoplasmic regulation of ADAM22 to activate TGF-β/Smad signaling. Int J Biol Sci 2026;22(8):3969–3989. DOI: 10.7150/ijbs.126013, PMID: 42088439.

[54] Yang J, Fu Z, Chen F, Vijaya Kumar S, Yang F, Zheng Y, *et al*. GLS1 Orchestrates Exosome-Mediated Tumor-Endothelial Communication to Facilitate Angiogenesis. Adv Sci (Weinh) 2026; 13(41):e75510. DOI: 10.1002/advs.75510, PMID: 42070227.